Chemical and Physical Properties of Sulfated Silk Fabrics

P. Taddei,[†] C. Arosio,[‡] P. Monti,[†] M. Tsukada,[§] T. Arai,[§] and G. Freddi*[,‡]

Centro di Studio sulla Spettroscopia Raman, Dipartimento di Biochimica "G. Moruzzi", Università di Bologna, via Belmeloro 8/2, Bologna 40126, Italy, Stazione Sperimentale per la Seta, via G. Colombo 83, 20133 Milano, Italy, and Organization of National Institute of Agrobiological Sciences, Oowashi 1-2, Tsukuba, Ibaraki 305-8634, Japan

Received October 24, 2006; Revised Manuscript Received January 19, 2007

Silk fabrics were treated with chlorosulphonic acid in pyridine for different times. The amount of sulfur bound to silk increased during the first 2 h of reaction and then reached a plateau. The amino acidic pattern of sulfated silk remained essentially unchanged for short reaction times ($\leq$2 h). Longer reaction times resulted in drastic changes in the concentration of Asp, Glu, and Tyr. Surface morphology and texture of silk fabrics changed upon sulfation. Warp and weft yarns became progressively thinner, and deposits of foreign material appeared on the fiber surface. Changes were more evident at longer reaction times ($\geq$2 h). Spectroscopic analyses performed by FT-IR and FT-Raman showed the appearance of new bands attributable to various vibrations of sulfated groups. The IR bands at 1049 and 1014 cm^{-1}, due to organic sulfate salts, were particularly intense. Bands assigned to alkyl sulfates and sulfonamides appeared in the 1300−1180 cm^{-1} range. Organic covalent sulfates displayed a weak but distinct IR band at 1385 cm^{-1}. Both IR and Raman spectra revealed that silk fibroin mainly bound sulfates through the hydroxyl groups of Ser and Tyr, while involvement of amines could not be proved. Changes observed in the amide I and II range indicated an increase of the degree of molecular disorder of sulfated silk. Accordingly, the I_{850}/I_{830} intensity ratio between the two Tyr bands at 850−830 cm^{-1} increased from 1.41 to 1.52, indicating a more exposed state of Tyr residues in sulfated silk. TGA, DSC, and TG analyses showed that sulfated silk attained a higher thermal stability. A thermal transition attributable to sulfated silk fibroin fractions appeared at about 260 °C in the DSC thermograms.

1. Introduction

The raw silk fibers produced by the *Bombyx mori* silkworm species are composed of inner filaments of a fibrous protein, fibroin, embedded in an outer coating formed by another protein (i.e., sericin). As a fiber, silk is a precious starting material for the textile industry. Degummed (i.e., sericin-deprived silk) is also a versatile and chemically reactive biopolymer possessing a range of excellent properties. It displays a very good ability to be functionalized and to have its structure and morphology modulated to match a wide range of functions. For these reasons, in recent years, the unique chemical, mechanical, physiological, and biological properties of silk have made this protein polymer highly attractive for developing innovative, knowledge-based multifunctional materials for different end-uses, which mainly fall within the scope of biomedical devices (i.e., scaffolds for tissue engineering).[1] According to the literature, silk fibroin has demonstrated an excellent biocompatibility.[2−4] As a biomaterial, it is easily tolerated, integrated into the regenerating tissue, and only slowly resorbed with time. Silk threads have been used for years and are still used as surgical stitches. Because of its ability to promote cell adhesion and growth, silk fibroin has been the object of an increasing interest as a potential biomaterial forming the core or coating the surfaces of scaffolds aimed at tissue engineering/regeneration/repair purposes. Silk fibers have been proposed for the preparation of various kinds of medical devices, such as polymer−hydroxyapatite composites for bone regeneration,[5] wire ropes for the substitution of the anterior cruciate ligament,[6] protective gauzes for the treatment of skin burns with improved blood compatibility,[7] and non-woven fibers for dermo-epidermal tissue regeneration.[8] Silk films, which can be easily prepared by casting an aqueous silk fibroin solution at room temperature, are highly attractive for their permeability to oxygen and water vapor and for the ability to support adhesion and growth of rodent fibroblasts and several types of normal adult human cells, including keratinocytes, fibroblasts, osteoblasts, endothelial cells, and astrocytes.[9−15]

Incorporation of sulfate and sulfonate groups into polymers is known to impart anti-coagulant and anti-thrombogenic activity on them. Gotoh et al.[16] investigated the anti-HIV and anti-coagulant activity of sulfated silk fibroin peptides and addressed their application as AIDS-preventing compounds. They found that sulfated silk fibroin peptides, obtained from degummed silk fibers by treatment with chlorosulphonic acid in pyridine, were able to completely block virus binding to cells in vitro and also to abolish cell-to-cell transmission and cell-free virus infection. The anti-HIV activity, which was associated to low cytotoxicity and weak anti-coagulant activity, allowed authors to propose sulfated silk fibroin peptides as an anti-AIDS component for vaginal anti-HIV formulations. More recently, Tamada et al.[17−19] studied the sulfation of silk fibroin and sericin with sulfuric acid or chlorosulphonic acid in pyridine and focused attention on the anti-coagulant properties of sulfated peptides. Silk fibroin peptides sulfated with sulfuric acid exhibited anti-coagulant activity, while unmodified silk fibroin did not.[17] However, the activity was 40-fold lower than that of heparin, a natural anti-coagulant widely applied in medicine, owing to the much lower content of sulfate groups. When sulfated silk fibroin peptides

* To whom correspondence should be addressed. Tel.: +39 02 2665990. Fax: +39 02 2362788. E-mail: freddi@ssiseta.it.

[†] Università di Bologna.

[‡] Stazione Sperimentale per la Seta.

[§] Organization of National Institute of Agrobiological Sciences.

10.1021/bm061017y CCC: $37.00
Published on Web 03/06/2007

were prepared by reaction with chlorosulphonic acid in pyridine, the efficiency of sulfation increased very much, and the anticoagulant activity increased as well, indicating that it strongly depends on the amount of sulfate groups incorporated into the protein.[18]

The biological properties and medical utility of sulfated polymers,[18] including the carbohydrate heparin,[20] are well-established. With reference to sulfated proteins and their role in leaving systems, Moore[21] reported that many proteins expressed in various mammalian cells and tissues undergo post-translational sulfation of the Tyr side chain (O-sulfation) and that most proteins comprising O-sulfated Tyr residues are secretory and trans-membrane proteins. Although the biological functions of this class of biopolymers is still poorly understood, it has emerged that sulfation clearly plays a key role in protein−protein interactions (i.e., optimal receptor−ligand interactions, proteolytic processing, and proteolytic activation of extracellular proteins).

In view of widening the biomedical utility of silk as a biomaterial, it is of interest to explore various chemical modification approaches able to complement the intrinsic outstanding properties of silk and to enhance its end-use performance. For example, effective antimicrobially active silk fibers were obtained by pretreating silk with tannic acid or ethylenediaminotetraacetic dianhydride, followed by formation of metal complexes with silver, copper, and cobalt.[22] Silk fibroin−lactose conjugates behaved as a scaffold for hepatocyte attachment.[23] Covalent decoration of silk films with integrin recognition sequences (RGD) resulted in a stimulation of osteoblast based mineralization in vitro.[13] The purpose of this study is to explore whether sulfation can be used as a tool to produce functional silk substrates applicable in the medical field. Sulfated silk fibroin peptides prepared by Tamada[17,18] were small in size and water soluble because sulfation was carried out for several hours, until the silk fiber was almost completely disintegrated. Conversely, our aim is to prepare sulfated silk fibers by keeping the intrinsic fiber properties and texture unchanged. To this purpose, short reaction times were selected, and fibers were sulfated with chlorosulphonic acid in pyridine, which is known to enhance the yield of sulfation.[18] Susceptibility of the reactive sites of silk fibroin to form sulfate salts was investigated. Surface morphology, physical structure, and thermal behavior of sulfated silk substrates were characterized by means of different analytical techniques (SEM, FT-IR, Raman, DSC, TMA, and TG).

2. Materials and Methods

2.1. Materials. Reagent grade pyridine (Cat. No. 166-05316) and chlorosulphonic acid (Cat. No. 038-2922) were purchased from Wako Pure Chemical Industries, Ltd. and were used without further purification. The *B. mori* silk fabric (Habutae, ca. 75 g/m^2) was treated in a glass flask with a solution prepared by adding 2.5 mL of chlorosulphonic acid to 15 mL of pyridine. The reaction system was gradually heated to 80 °C in a thermostatically controlled bath and kept at constant temperature for different times (1−4 h). At the end of the reaction, samples were washed with isopropanol, then with acetone at 55 °C for 1 h to remove reagents, and finally with tap water. Samples were kept under standard atmosphere (20 °C, 65% relative humidity) before subsequent analysis.

2.2. Amino Acid Analysis. The amino acid composition of silk fabrics was determined after acid hydrolysis with 6 N HCl, at 105 °C for 24 h, under vacuum. Free amino acids were analyzed by HPLC (AccQ-Tag Method, Waters), at a flow rate of 1 mL/min. Eluate was detected at 254 nm. Samples were analyzed in duplicate. The quantitative amino acid composition was determined by external standard calibration (Amino Acid Standard H, Pierce).

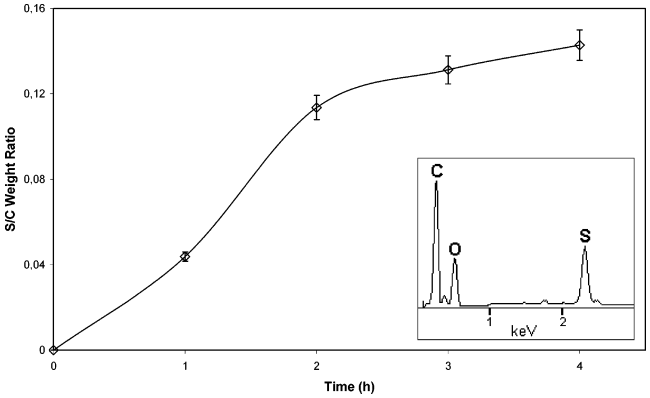

Figure 1. Time dependence of sulfur content in silk fabrics sulfated with chlorosulphonic acid in pyridine. The sulfur content was expressed as a ratio between the intensity of sulfur and the intensity of carbon lines. Results are the average of at least three spectra. The insert shows a typical EDX spectrum with Kα lines for carbon (0.28 keV), oxygen (0.52 keV), and sulfur (2.31 keV).

2.3. Mechanical Properties. Mechanical properties were determined according to the UNI-EN-ISO 2062 standard method by means of an Instron tensile testing machine model 4501, at a 50 mm gauge length and 50 mm/min crossbar rate. Measurements were performed under standard conditions of temperature (20 °C) and humidity (65%). Values of breaking strength and elongation at break were the average of 10 individual measurements.

2.4. Scanning Electron Microscopy (SEM). Surface morphology of silk fabrics was examined by means of scanning electron microscopy (SEM), using a Jeol microscope JSM-6380LV. Samples were observed at 10 keV acceleration voltage, after gold coating under reduced argon atmosphere with a Med 020 Coating System (BAL-TEC). EDX spectra were acquired on carbon coated samples at 20 keV with a EDS 2004 X-ray detector (IXRF Systems, Inc.) connected to the Jeol microscope JSM-6380LV.

2.5. FT-IR Spectroscopy. IR spectra of the finely cut samples were measured on a Jasco FT-IR 300E spectrophotometer using KBr pellets (about 0.5% w/w). The spectral resolution was 4 cm^{-1}. The spectra of the same sample recorded on different KBr pellets were practically coincident.

2.6. FT-Raman Spectroscopy. Raman spectra were recorded on a Bruker IFS66 spectrometer equipped with a FRA-106 FT-Raman module and a cooled Ge-diode detector. The excitation source was a Nd^{3+}/YAG laser (1064 nm) in the backscattering (180°) configuration. The focused laser beam diameter was about 100 μm, the spectral resolution was 4 cm^{-1}, and the laser power at the sample was about 150 mW. Raman spectra were recorded on several different points of the specimens to check for homogeneity. The spectra were practically coincident, indicating that the samples were compositionally homogeneous.

2.7. Thermomechanical Analysis (TMA). TMA was carried out using a Rigaku Denki instrument at a heating rate of 10 °C/min. TMA full scale was ±500 μm.

2.8. Differential Scanning Calorimetry (DSC). DSC measurements were performed with a DSC-10 instrument (Rigaku Denki), from room temperature to 500 °C, at a heating rate of 10 °C/min, on 2−3 mg samples. The open aluminum cell was swept with dry N_2 during the analysis.

2.9. Thermogravimetric Analysis (TG). TG was performed with a TGA Q500 instrument (TA Instruments), from room temperature to 550 °C, at a heating rate of 20 °C/min, on 3 mg samples. The cell was swept with N_2 during the analysis.

Table 1. Amino Acid Composition (μmol/mg) of Control and Sulfated Silk Fabrics Treated for Different Times

AA	control (μmol/mg ± SD)	S1[a] (μmol/mg ± SD)	S2[a] (μmol/mg ± SD)	S3[a] (μmol/mg ± SD)	S4[a] (μmol/mg ± SD)
Asp	194 ± 5	213 ± 1	201 ± 5	64 ± 5	71 ± 1
Ser	1529 ± 33	1524 ± 4	1524 ± 5	1830 ± 126	1610 ± 74
Glu	117 ± 2	125 ± 1	120 ± 4	51 ± 4	45 ± 3
Gly	5926 ± 175	5791 ± 27	5876 ± 83	6250 ± 384	7140 ± 254
His	74 ± 8	78 ± 3	81 ± 2	63 ± 1	78 ± 9
Arg	77 ± 3	71 ± 1	77 ± 3	92 ± 5	76 ± 2
Thr	128 ± 3	123 ± 2	125 ± 4	129 ± 7	88 ± 7
Ala	3542 ± 7	3698 ± 1	3639 ± 36	3769 ± 202	4217 ± 143
Pro	64 ± 1	65 ± 1	64 ± 2	78 ± 7	85 ± 1
Cys	n.d.	n.d.	n.d.	n.d.	n.d.
Tyr	772 ± 30	740 ± 2	749 ± 12	572 ± 43	244 ± 7
Val	308 ± 3	294 ± 22	304 ± 2	277 ± 19	223 ± 9
Met	7 ± 1	11 ± 1	n.d.	n.d.	n.d.
Lys	40 ± 1	42 ± 1	39 ± 1	39 ± 3	34 ± 2
Ile	87 ± 1	88 ± 1	86 ± 1	99 ± 7	75 ± 4
Leu	72 ± 1	73 ± 1	70 ± 1	48 ± 3	58 ± 2
Phe	101 ± 4	99 ± 1	101 ± 1	83 ± 8	89 ± 3

[a] Reaction time with chlorosulphonic acid in pyridine: S1 = 1 h; S2 = 2 h; S3 = 3 h; and S4 = 4 h.

3. Results and Discussion

3.1. Chemical and Mechanical Characterization. Reitz et al.[24] first reported the sulfation of silk fibroin with chlorosulphonic acid in pyridine. They studied the chemistry of the reaction, with emphasis on the identification of the amino acid side groups taking part in the reaction, and were able to demonstrate that aliphatic and phenolic hydroxyl, thiol, amine, guanidyl, and indole groups were transformed into sulfates and sulfamates. Sulfation of silk fabric under the conditions detailed in the Materials and Methods resulted in an increase in weight attributable to the introduction of sulfate groups into the fiber matrix. However, the calculation of the weight gain was not considered a suitable method to evaluate the yield of reaction because it is well-known that silk fibroin may undergo more or less extensive degradation by cleavage of peptide bonds and release of soluble peptides.[18] The SEM-EDX technique was therefore adopted to follow the extent of sulfation of silk as a function of the reaction time. The graph of Figure 1 shows that the amount of sulfur bound to silk fibers increased steadily during the first 2 h and then tended to a plateau for longer reaction times. These results indicate that a reaction time of 2 h is suitable to attain a relatively high degree of sulfation. Longer treatment times may lead to a further increase of sulfur content, but the risk of extensive fiber degradation becomes very high because the pyridine−chlorosulphonic acid reaction system is able to hydrolyze silk fibroin.[18]

Amino acid analysis was used as a probe to detect changes in the chemical structure of sulfated silk fibroin. Table 1 lists the amino acid composition of sulfated silk samples, while Figure 2 shows the trend of amino acids as a function of the reaction time, from 1 to 4 h (samples S1, S2, S3, and S4, respectively). The amino acidic pattern of samples S1 and S2 is closely similar to that of the control sample. With increasing the reaction time up to 4 h, the concentration of Gly, Ala, and, to lower extent, Ser tended to increase. On the other hand, all the other amino acids, especially Tyr and acidic ones (Asp, Glu), decreased. These results indicate that silk fibroin underwent severe hydrolytic degradation at longer reaction times. In particular, amorphous amino acid sequences comprising acidic and phenolic amino acid residues, as well as other amino acids with bulky and polar side chains, were probably more prone to degradation under the reaction conditions adopted. Cleavage of peptide bonds and solubilization of peptide fragments were probably responsible for the loss of some amino acids and consequent enrichment of others. It is also interesting to note that the amino acid chromatograms of samples S3 and S4 displayed additional nonidentified peaks attributable to sulfur adducts and/or degradation products, which may account for the observed changes in the amino acid composition.

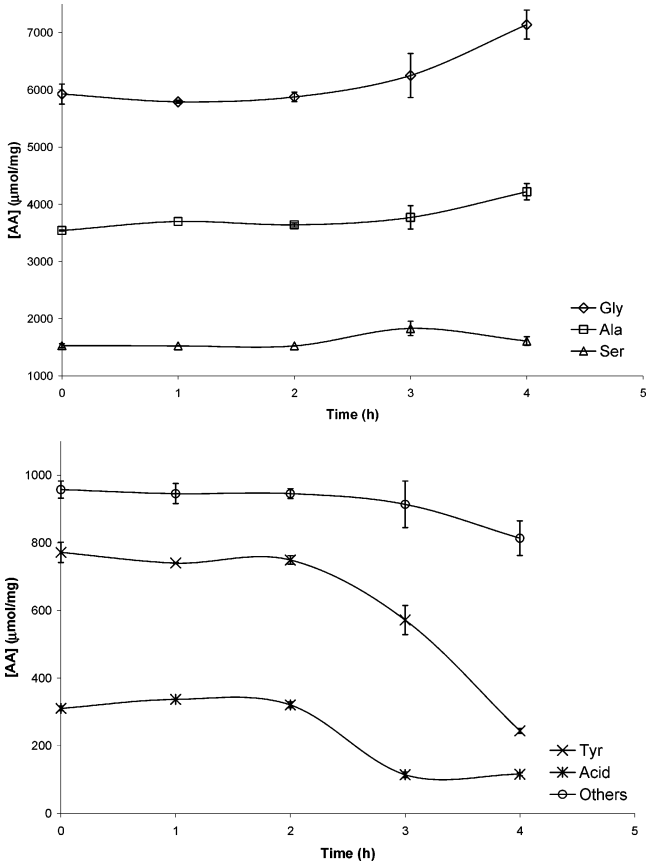

Figure 2. Behavior of amino acids as a function of the time of sulfation (data from Table 1).

The effect of sulfation on the mechanical properties of silk fibers is shown in Figure 3. The chemical treatment induced a decrease of both strength and elongation at break. The average loss of strength ranged from 20 to 35% after 1 or 2 h of reaction time, respectively. The average loss of elasticity was about 35%.

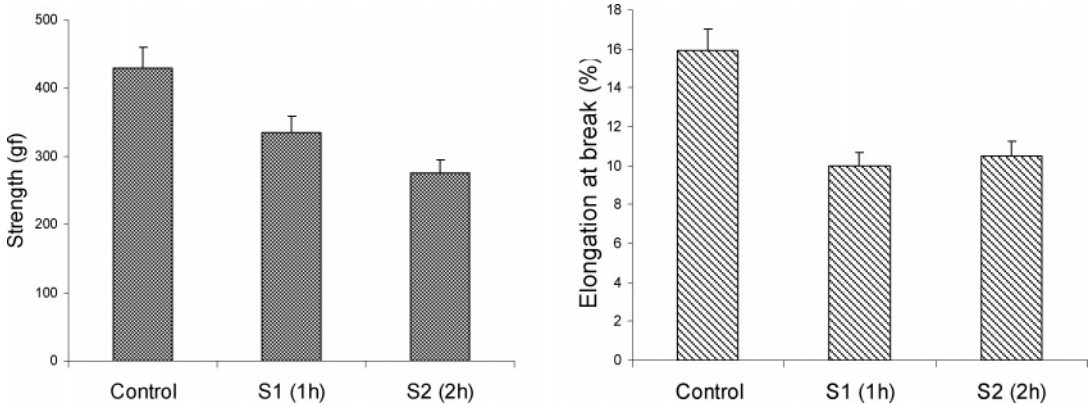

Figure 3. Mechanical properties of sulfated silk fibers.

This level of tensile performance can still be considered compatible with end-use requirements where silk is not subjected to strong and/or prolonged stresses. Longer reaction times (i.e., >2 h) resulted in a dramatic loss of tensile performance. The accumulated chemical and tensile results confirm that short reaction times (≤2 h) are the best choice in terms of both degree of sulfation and chemical and mechanical integrity of silk fibers.

3.2. Morphological Characterization. Morphological properties of silk fabrics after sulfation were analyzed by SEM. Figure 4 shows the pictures of untreated and sulfated silk fabrics with different degrees of sulfation. The series of low magnification pictures clearly indicate that the texture of the fabric was drastically changed by the treatment. Both warp and weft yarns became progressively thinner and more compact as though the silk fibroin filaments forming the individual yarns were glued to each other. As a consequence, voids began appearing at the yarn crossover. Pictures at higher magnification showed the presence of foreign materials on the fiber surface. In some cases, deposits showed a regular shape as though they were of mineral origin (sample S2). The longer the reaction time, the higher the amount of foreign materials. The results of the morphological characterization supplement the chemical and mechanical analyses, indicating that short treatment times are safer for both maintaining the intrinsic chemical structure of silk and keeping the texture of the fabric unchanged. Moreover, the results indicate that the cleaning procedure after sulfation needs further improvement to remove any undesired foreign material that might compromise the subsequent utilization of sulfated silk substrates in biomedical applications. In fact, the presence of foreign deposits may lead to adverse interactions with the biological environment, such as unwanted deposition of proteins and/or thrombus formation.

3.3. FT-IR and Raman Spectroscopy Analyses. Figure 5 shows the IR spectra of sulfated silk fabrics. The spectrum of untreated silk, reported for comparison purposes, is characterized by a well-defined strong peak at 1703 cm^{-1} in the amide I range, attributed to the antiparallel β-sheet conformation, and a broad band centered at about 1645 cm^{-1}. In the amide II region, a distinct maximum at 1514 cm^{-1} was superimposed to a broad band centered at about 1540 cm^{-1}. Two amide III bands were observed at 1260 and 1228 cm^{-1}. The degree of crystallinity, expressed as the intensity ratio of the two amide III bands, was similar to that reported by Bhat and Nadiger[25] for *B. mori* silk ($I_{1260}/I_{1228} = 0.63$ from Figure 5). These spectral features, together with the position of the amide V band at 695 cm^{-1}, revealed that silk fibers in the fabric have a prevalent β-sheet structure.

Upon sulfation, new bands attributable to various sulfated groups appeared and became progressively stronger at increasing reaction times. These bands are reported in Table 2 together with their tentative assignments. Among them, the new strong absorptions appearing at 1049 and 1014 cm^{-1} are attributed to vibrations of organic sulfate salts.[26−28] Sulfation also resulted in a progressive increase in intensity and broadening of the bands in the 1300−1180 cm^{-1} range, where $\nu_{as}SO_2$ of alkyl sulfate salts,[26,27] $\nu_{as}SO_2$ of sulfonamides,[26,29] and ν_sSO_2 of organic covalent sulfates[30] fall and overlap the amide III band of silk. Moreover, in the spectrum of sample S3, a new band appeared at 1385 cm^{-1}, attributable to the $\nu_{as}SO_2$ mode of organic covalent sulfates.[26,30]

The IR spectra showed that some conformational changes occurred by the effect of sulfation. The amide I component at 1645 cm^{-1} increased in intensity with respect to that at 1703 cm^{-1}. Accordingly, the intensity of the amide II component at 1540 cm^{-1} increased with respect to that at 1514 cm^{-1}. This trend is consistent with an increase of the degree of disorder in sulfated silk fibers. In fact, it has been reported that *B. mori* silk in the random coil conformation displays amide I and II modes at about 1650 and 1540 cm^{-1}, respectively.[31] It must be observed that the intensity of the IR amide I band at about 1645 cm^{-1} might have been enhanced by the presence of different amounts of water absorbed by the samples. Nevertheless, the trends of amide II in IR and amide III in Raman led us to conclude that sulfation caused an increase of the degree of disorder of silk fibers.

Raman spectroscopy results are consistent with the previous IR findings. Figure 6 compares the Raman spectra of untreated and sulfated silk (sample S3). With reference to our previous Raman studies on *B. mori* silk fibroin in film and fiber forms,[32] the position of the amide I (1665 cm^{-1}) and amide III (1264 and 1229 cm^{-1}) modes confirms the prevailing β-sheet conformation of both untreated and sulfated silk. However, the change in the relative intensity of the two amide III components, with that at 1229 cm^{-1} decreasing with respect to that at 1264 cm^{-1}, indicates that the degree of molecular disorder increased upon sulfation. Actually, *B. mori* silk fibroin in the random coil conformation displays an amide III band at 1265 cm^{-1}.[33]

As compared to IR, the Raman spectra underwent minor changes upon sulfation. Nevertheless, new bands due to sulfate groups were detectable at 575 and 622 cm^{-1} (attributable to δSO_3 according to IR assignments reported in Table 2) and between 1100 and 1000 cm^{-1}, where four bands in the shoulder form can be identified. Those at 1065, 1055, and 1025 cm^{-1} can be attributed to ν_sSO_2 of different sulfate residues, in agreement with the spectrum of heparin,[29,34] while that at 1015 cm^{-1} is attributable to νCO of organic sulfated salts.[27,28] Moreover, the band at 1158 cm^{-1} (νCC, νCOH)[33] increased in intensity and shifted to 1164 cm^{-1} because of the possible

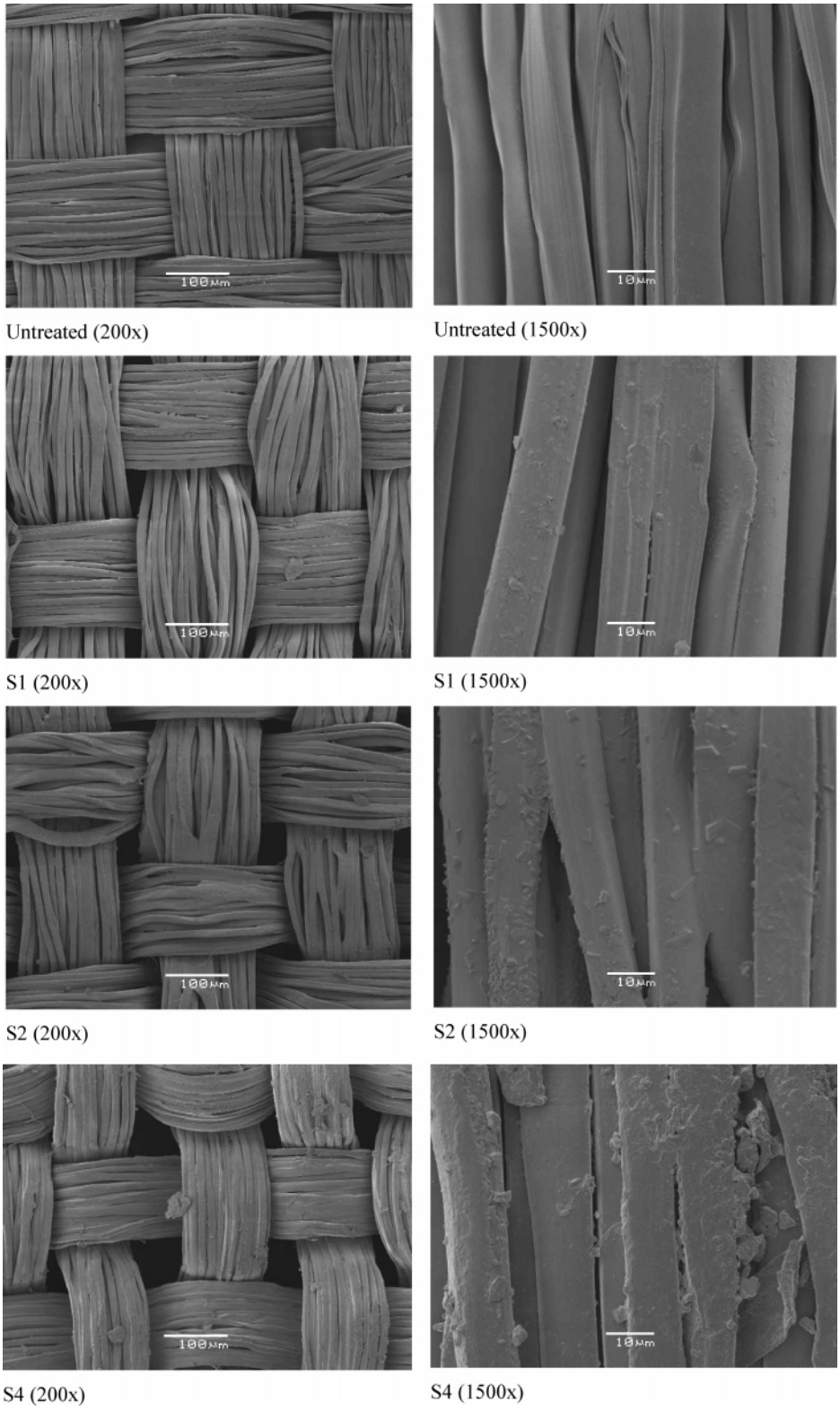

Figure 4. SEM pictures of untreated and sulfated silk fabrics. Reaction time with chlorosulphonic acid in pyridine: S1 = 1 h; S2 = 2 h; and S4 = 4 h. Low (200×) and high (1500×) views are shown for each sample.

contribution of the $\nu_s SO_2$ mode of sulfonamides.[35] The corresponding $\nu_{as} SO_2$ mode of sulfonamides, which is quite variable in intensity and often hardly detectable, could contribute to the strengthening and broadening of the set of bands centered at about 1320 cm^{-1}.[35]

The IR and Raman spectral features clearly point out the formation of organic sulfate salts by reaction of silk fibroin with chlorosulphonic acid in pyridine. The sulfate groups were covalently bound through the hydroxyl group of tyrosine (Tyr) and serine (Ser). Interestingly, no bands attributable to foreign materials (inorganic salts) were detected. It is worth noting that the IR band at 1385 cm^{-1} may be considered indicative of the formation of organic covalent sulfates with a high extent of sulfation, likely attributable to cross-linking of fibroin chains, which could explain the formation of an insoluble fraction during the sulfation reaction as reported by Tamada.[18] The involvement

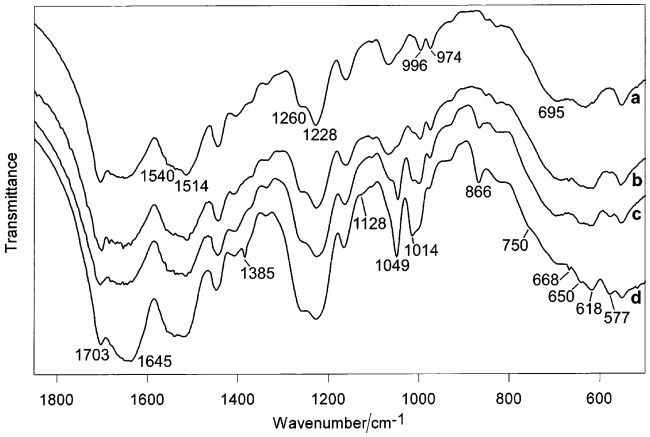

Figure 5. FT-IR spectra of untreated (a) and sulfated silk fabrics. Reaction time with chlorosulphonic acid in pyridine: (b) S1 = 1 h; (c) S2 = 2 h; and (d) S3 = 3 h.

Table 2. Wavenumbers (cm^{-1}) and Assignments of the IR Bands Attributable to Sulfate Groups in Sulfated Silk Samples (See Figure 3)

wavenumbers (cm^{-1})	assignments	refs
577		
618	δSO_3	27, 28, 31
650		
668		
750 sh[a]	ν_sS-O-C	27, 28
866	ν_{as}S-O-C	27, 31
1014	νCO organic sulfate salts	28, 29
1049	$\nu_s SO_2$ aromatic sulfate salts	27, 28
1128 sh[a]	$\nu_s SO_2$ primary alkyl sulfate salts	27
1180−1300	$\nu_{as} SO_2$ alkyl sulfate salts	27, 28
	$\nu_{as} SO_2$ sulfonamides	27, 30
	$\nu_s SO_2$ organic covalent sulfates	31
1385[b]	$\nu_{as} SO_2$ organic covalent sulfates	27, 31

[a] sh = shoulder. [b] Detectable only in the spectrum of the sample S3 (reaction time = 3 h).

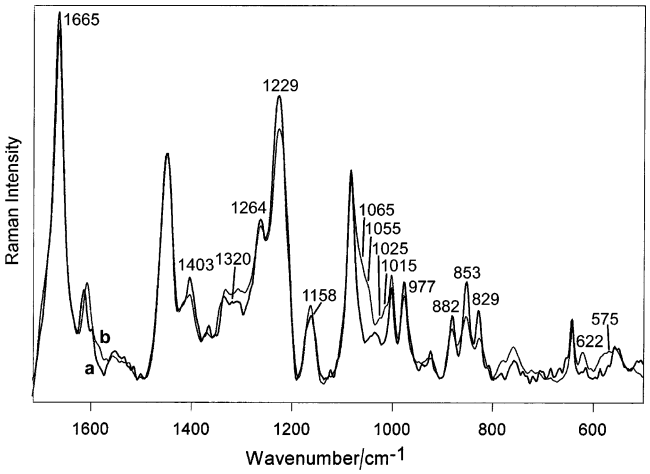

Figure 6. FT-Raman spectra of silk fabrics untreated (a) and sulfated by reaction with chlorosulphonic acid in pyridine for 3 h (b).

of the amine groups of basic amino acid residues in the reaction is not easily detectable. Nevertheless, the increased intensity of the Raman band at 1164 cm^{-1} may reasonably account for sulfation of amines as well.

The IR spectra reported by Tamada[18] were significantly different from those reported in this paper. The former showed only a strong band near 1200 cm^{-1}, generically attributed to SO_2 groups, and did not display the bands in the 1100−800 cm^{-1} range, attributable to vibrations of organic sulfate salts. Therefore, the materials characterized in our work are significantly different from those obtained by Tamada.[18]

Table 3. Temperatures of the Main Thermal Transition Detected by TMA, DSC, and TG on Control and Sulfated Silk Fabrics

	TMA (T (°C))	DSC (T (°C))		TG (T (°C))	
control	300		314		327
S1[a]		≈260	324		331
S2[a]	310	250−266	326	≈260	337
S3[a]	308	248−272	330	≈260	327

[a] Reaction time with chlorosulphonic acid in pyridine: S1 = 1 h; S2 = 2 h; and S3 = 3 h.

The loss of intensity of a series of Raman bands, including amide I and III bands, those at 1403 cm^{-1} ($\delta_{as}[C(CH_3)_2]$), 977 cm^{-1} (ρCH_3), 882 cm^{-1} (ρCH_2), which are related to vibrations of CH groups,[33] and the doublet at 850−830 cm^{-1} due to Tyr residues (Fermi resonance between the ring breathing vibration and the overtone of an out-of-plane ring bending vibration),[36] suggests that silk degradation probably occurred upon sulfation. The intensity ratio between the two Tyr bands at 850−830 cm^{-1} (I_{850}/I_{830}) is sensitive to the hydrogen bonding state of the Tyr phenoxyl group and has been extensively used as an indicator of Tyr interactions in globular proteins, their assemblies, and their degree of exposure to water.[36] In fact, if the Tyr residue is buried, the phenolic OH group acts as a strong hydrogen bond donor to an electronegative acceptor (such as carboxyl oxygen), and the I_{850}/I_{830} ratio achieves its minimum value of about 0.3.[37] When the Tyr residue is on the surface of a protein in aqueous solution (exposed), the phenolic OH group acts as both a donor and an acceptor of moderate strength hydrogen bonds, and I_{850}/I_{830} is approximately 1.25.[37] When the phenoxyl oxygen is the acceptor of a strong hydrogen bond from an electropositive group (such as a lysyl NH_3^+ group) and does not participate in significant hydrogen bond donation, I_{850}/I_{830} approaches the presumed maximum value of 2.5.[37] This correlation was refined on the basis of the results on filamentous virus capsids[38−41] and silk fibroin in the silk I form,[42] for which an I_{850}/I_{830} ratio exceeding the latter value was found. This feature was interpreted as indicative of a highly hydrophobic local environment for Tyr residues, a state not represented in any previously studied globular protein. Actually, the value of the intensity ratio reflects the average environment experienced by all the Tyr residues present in the protein. The I_{850}/I_{830} intensity ratio increased from 1.41 to 1.52 upon sulfation, suggesting a change toward a more exposed state of Tyr residues in sulfated fibroin. This feature is in agreement with a more disordered conformation detected by both IR and Raman spectroscopy.

3.4. Thermal Properties. Various analytical techniques were used to investigate the thermal behavior of sulfated silk fibers (i.e., TMA, DSC, and TG). The temperature of the most significant thermal events recorded by TMA, DSC, and TG are listed in Table 3, which summarizes the main finding obtained in this part of the study. In particular, the values of the temperature obtained from TMA analysis refer to the onset of the final abrupt extension leading to fiber breaking.[43] Before this event, both reference and sulfated fibers behaved similarly, showing a gradual contraction of about 0.6% from room temperature to 150 °C, followed by a progressive extension until about 250 °C, during which the initial fiber length was recovered (curves not shown). Sulfation resulted in an upward shift of the limit temperature of fiber breakage, suggesting a slight but significant contribution of the treatment to the thermomechanical

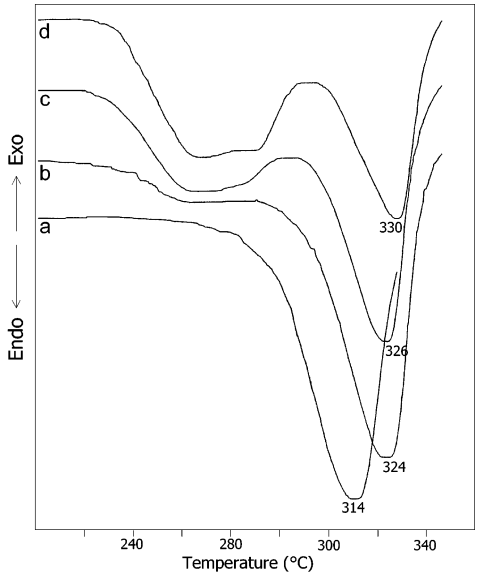

Figure 7. DSC thermograms of untreated (a) and sulfated silk fabrics. Reaction time with chlorosulphonic acid in pyridine: (b) S1 = 1 h; (c) S2 = 2 h; and (d) S3 = 3 h.

stability of silk fibers. Similar results were reported for silk treated with alkali[44] or grafted with vinyl monomers.[45−47]

DSC curves of sulfated silks are shown in Figure 7. Values of the peak temperature of the main thermal transitions occurring in the range from 200 °C until thermal degradation are listed in Table 3. The high temperature peak (>300 °C) is attributed to the thermal degradation of silk fibroin with an oriented β-sheet structure.[48] Following sulfation, this peak shifted to a higher temperature of about 10−15 °C. The reference sample did not show any trace of thermal transitions at lower temperature, while sulfated silks displayed a broad endothermic event falling at about 260 °C, which assumed a clear bimodal shape with increasing the extent of sulfation. Actually, the precise attribution of this transition is a very difficult task. The observation that the intensity is directly related to the extent of sulfation suggests that it might involve fiber domains comprising the sulfated amino acid residues, which were probably destabilized and became more sensitive to the thermal treatment. In fact, an increase of the degree of molecular disorder of sulfated silk fibers was clearly evidenced by IR and Raman spectroscopy analyses. Breakage of the cross-links formed into the silk fibroin matrix by action of covalently bound sulfates might have contributed to the thermal transition at around 260 °C as well.

DSC results were essentially confirmed by TG analysis (Figure 8). The kinetics of weight loss as a function of temperature revealed the presence of two subsequent degradation phenomena, a broad and weaker one occurring at about 260 °C and a strong one at above 300 °C. The latter, which corresponds to the DSC thermal degradation peak, moved to higher temperatures upon sulfation. This feature confirms that the most ordered and crystalline fiber domains, into which the sulfate groups could hardly penetrate, gained an intrinsically higher thermal stability as though the sulfated silk fibroin fractions in which they are embedded exerted a protective effect against heat.

4. Conclusion

Silk fabrics treated with chlorosulphonic acid in pyridine bound different amounts of sulfate mainly through the hydroxyl groups of Ser and Tyr. The amount of bound sulfur increased during the first 2 h of reaction and then remained almost

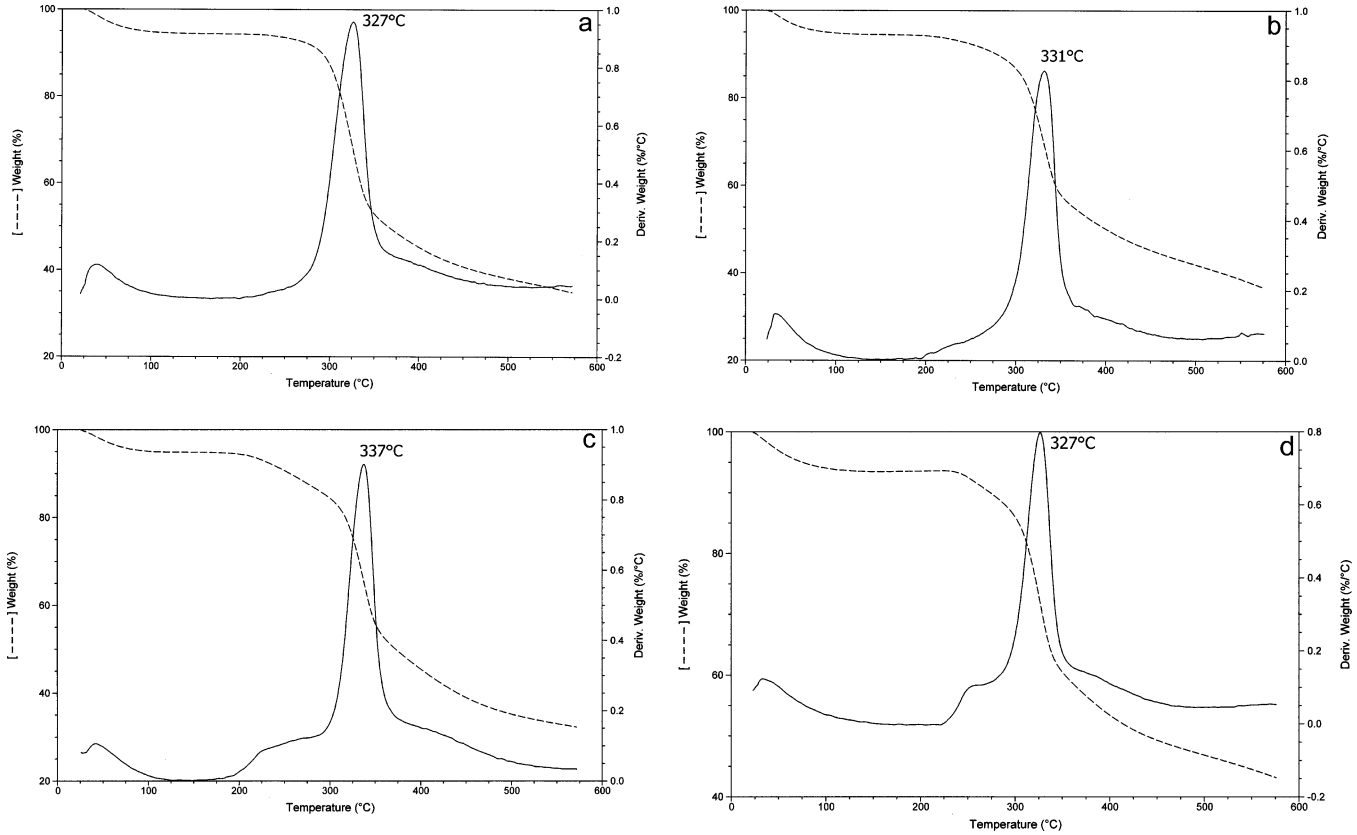

Figure 8. TG curves of silk fabrics untreated (a) and sulfated with chlorosulphonic acid in pyridine: (b) S1 = 1 h; (c) S2 = 2 h; and (d) S3 = 3 h. Broken line: weight loss and solid line: first derivative.

constant. Chemical degradation, as well as strong changes in surface morphology and texture of silk fabrics, appeared at reaction times longer than 2 h. Details about the chemistry of the reaction and the effect of sulfation on the structure and physical properties of silk were provided by amino acid analysis, FT-IR and FT-Raman spectroscopy, and thermal analyses. Interestingly, sulfated silks attained a significantly higher thermal stability.

The accumulated results indicate that long treatment times (>2 h) should be avoided because the amount of bound sulfur does not increase too much while the risk of extensive fiber degradation becomes very high because the pyridine−chlorosulphonic acid reaction system is able to hydrolyze silk fibroin. In fact, an essential requirement for further application of sulfated silk fabrics is to maintain the physical−chemical structure and texture of silk as much as possible.

The results obtained in this study will form a frame of knowledge for further biological investigations aimed at demonstrating the biomedical utility of sulfated silk. The recognized biomedical utility of sulfated polymers seems to suggest a possible exploitation of sulfation as a tool to produce functional silk substrates applicable in the medical field.

Acknowledgment. This work was supported by ex-60% grants from MIUR, Italy.

References and Notes

(1) Altman, G. H.; Diaz, F.; Jakuba, C.; Calabro, T.; Horan, R. L.; Chen, J.; Lu, H.; Richmond, J.; Kaplan, D. L. Silk-based biomaterials. *Biomaterials* **2003**, *24*, 401−416.

(2) Sakabe, H.; Ito, H.; Miyamoto, T.; Noishiki, Y.; Ha, W. S. In vivo blood compatibility of regenerated silk fibroin. *Sen'i Gakkaishi* **1989**, *45*, 487−490.

(3) Santin, M.; Motta, A.; Freddi, G.; Cannas, M. In vitro evaluation of the inflammatory potential of the silk fibroin. *J. Biomed. Mater. Res.* **1999**, *46*, 382−389.

(4) Panilaitis, B.; Altman, G. H.; Chen, J.; Jin, H. J.; Karageorgiu, V.; Kaplan, D. L. Macrophage response to silk. *Biomaterials* **2003**, *24*, 3079−3085.

(5) Furuzono, T.; Yasuda, S.; Kimura, T.; Kyotani, S.; Tanaka, J.; Kishida, A. Nano-scaled hydroxyapatite/polymer composite. IV. Fabrication and cell adhesion properties of the three-dimensional scaffold made of composite material with silk fibroin substrate to develop a percutaneous device. *J. Artif. Organs* **2004**, *7*, 137−144.

(6) Altman, G. H.; Horan, R. L.; Lu, H.; Moreau, J.; Martin, I.; Richmond, J.; Kaplan, D. L. Silk matrix for tissue engineered anterior cruciate ligament. *Biomaterials* **2002**, *23*, 4131−4141.

(7) Sugihara, A.; Sugiura, K.; Morita, H.; Ninagawa, T.; Tubouchi, K.; Tobe, R.; Izumiya, M.; Horio, T.; Abraham, N. G.; Ikehara, S. Promotive effects of a silk film on epidermal recovery from full-thickness skin wounds. *Proc. Soc. Exp. Biol. Med.* **2000**, *225*, 58−64.

(8) Dal Pra, I.; Freddi, G.; Minic, J.; Chiarini, A.; Armato, U. De novo engineering of reticular connective tissue in vivo by silk fibroin nonwoven materials. *Biomaterials* **2005**, *26*, 1987−1999.

(9) Minoura, N.; Tsukada, M.; Nagura, M. Physicochemical properties of silk fibroin membrane as a biomaterial. *Biomaterials* **1990**, *11*, 430−434.

(10) Minoura, N.; Aiba, S.; Gotoh, Y.; Tsukada, M.; Imai, Y. Attachment and growth of cultured fibroblast cells on silk protein matrices. *J. Biomed. Mater. Res.* **1995**, *29*, 1215−1221.

(11) Gotoh, Y.; Tsukada, M.; Minoura, N. Effect of the chemical modification of the arginyl residue in *Bombyx mori* silk fibroin on the attachment and growth of fibroblast cells. *J. Biomed. Mater. Res.* **1998**, *39*, 351−357.

(12) Inouye, K.; Kurokawa, M.; Nishikawa, S.; Tsukada, M. Use of *Bombyx mori* silk fibroin as a substratum for cultivation of animal cells. *J. Biochem. Biophys. Methods* **1998**, *37*, 159−164.

(13) Sofia, S.; McCarthy, M. B.; Gronowicz, G.; Kaplan, D. L. Functionalized silk-based biomaterials for bone formation. *J. Biomed. Mater. Res.* **2001**, *54*, 139−148.

(14) Chiarini, A.; Petrini, P.; Bozzini, S.; Dal Pra, I.; Armato, U. Silk fibroin/poly(carbonate)-urethane as a substrate for cell growth: in vivo interactions with human cells. *Biomaterials* **2003**, *24*, 789−799.

(15) Dal Pra, I.; Petrini, P.; Chiarini, A.; Bozzini, S.; Farè, S.; Armato, U. Silk fibroin-coated three-dimensional polyurethane scaffolds for tissue engineering: interactions with normal human fibroblasts. *Tissue Eng.* **2003**, *9*, 1113−1121.

(16) Gotoh, K.; Izumi, H.; Kanamoto, T.; Tamada, Y.; Nakashima, H. Sulfated fibroin, a novel sulfated peptide derived from silk, inhibits human immunodeficiency virus replication in vitro. *Biosci. Biotechnol. Biochem.* **2000**, *64*, 1664−1670.

(17) Tamada, Y. Sulfation of silk fibroin by sulphuric acid and anticoagulant activity. *J. Appl. Polym. Sci.* **2003**, *87*, 2377−2382.

(18) Tamada, Y. Sulfation of silk fibroin by chlorosulfonic acid and the anticoagulant activity. *Biomaterials* **2004**, *25*, 377−383.

(19) Tamada, Y.; Sano, M.; Niwa, K.; Imai, T.; Yoshino, G. Sulfation of silk sericin and anticoagulant activity of sulphated sericin. *J. Biomater. Sci., Polym. Ed.* **2004**, *15*, 971−980.

(20) Day, J. R. S.; Landis, R. C.; Taylor, K. M. Heparin is much more than just an anticoagulant. *J. Cardiothorac. Vasc. Anesth.* **2004**, *18*, 93−100.

(21) Moore, K. L. The biology and enzymology of protein tyrosine *O*-sulfation. *J. Biol. Chem.* **2003**, *278*, 24243−24246.

(22) Tsukada, M.; Arai, T.; Colonna, G. M.; Boschi, A.; Freddi, G. Preparation of metal-containing protein fibers and their antimicrobial properties. *J. Appl. Polym. Sci.* **2003**, *89*, 638−644.

(23) Gotoh, Y.; Niimi, S.; Hayakawa, T.; Miyashita, T. Preparation of lactose-silk fibroin conjugates and their application as a scaffold for hepatocyte attachment. *Biomaterials* **2004**, *25*, 1131−1140.

(24) Reitz, H. C.; Ferrel, R. E.; Fraenkel-Conrat, H.; Olcott, H. S. Action of sulphating agents on proteins as model substances. II. Pyridine-chlorosulfonic acid. *J. Am. Chem. Soc.* **1946**, *68*, 1031−1035.

(25) Bhat, N. V.; Nadiger, G. S. Crystallinity in silk fibers: partial acid hydrolysis and related studies. *J. Appl. Polym. Sci.* **1980**, *25*, 921−932.

(26) Socrates, G. In *Infrared Characteristic Group Frequencies*, 2nd ed.; Wiley: Chichester, 1980.

(27) Chihara, G. Medical and biochemical application of infrared spectroscopy. V. Infrared absorption spectra of organic sulfate esters. *Chem. Pharm. Bull.* **1960**, *8*, 988−994.

(28) Christe, K. O.; Curtis, E. C. The vibrational spectra of dimethyl sulfates. *Spectrochim. Acta, Part A* **1972**, *28*, 1889−1898.

(29) Cabassi, F.; Casu, B.; Perlin, A. S. Infrared absorption and Raman scattering of sulfate groups of heparin and related glycosaminoglycans in aqueous solution. *Carbohydr. Res.* **1978**, *63*, 1−11.

(30) Paulson, G.; Bakke, J.; Giddings, J.; Simpson, M. Mass and infrared spectra of diaryl and aryl alkyl sulfate diesters. *Biomed. Mass Spectrom.* **1978**, *5*, 128−132.

(31) Magoshi, J.; Mizuide, M.; Magoshi, Y.; Takahashi, K.; Kubo, M.; Nakamura, S. Physical properties and structure of silk. VI. Conformational changes in silk fibroin induced by immersion in water at 2−130 °C. *J. Polym. Sci., Polym. Phys. Ed.* **1979**, *17*, 515−520.

(32) Monti, P.; Freddi, G.; Bertoluzza, A.; Kasai, N.; Tsukada, M. Raman spectroscopic studies of silk fibroin from *Bombyx mori*. *J. Raman Spectrosc.* **1998**, *29*, 297−304.

(33) Edwards, H. G. M.; Farwell, D. W. Raman spectroscopic studies of silk. *J. Raman Spectrosc.* **1995**, *26*, 901−909 and literature cited therein.

(34) Atha, D. H.; Gaigalas, A. K.; Reipa, V. Structural analysis of heparin by Raman spectroscopy. *J. Pharm. Sci.* **1996**, *85*, 52−56.

(35) Dollish, F. R.; Fateley, W. G.; Bentley, F. F. In *Characteristic Raman Frequencies of Organic Compounds*; Wiley: New York, 1973.

(36) Tu, A. T. In *Raman Spectroscopy in Biology: Principles and Applications*; John Wiley and Sons, Ltd.: Chichester, 1982; literature cited therein.

(37) Siamwiza, M. N.; Lord, R. C.; Chen, M. C.; Takamatsu, T.; Harada, I.; Matsuura, H.; Shimanouchi, T. Interpretation of the doublet at 850 and 830 cm^{-1} in the Raman spectra of tyrosyl residues in proteins and certain model compounds. *Biochemistry* **1975**, *14*, 4870−4876.

(38) Overman, S. A.; Aubrey, K.; Vispo, N. S.; Cesareni, G.; Thomas, G. J., Jr. Novel tyrosine markers in Raman spectra of wild-type and mutant (Y21M and Y24M) Ff virions indicate unusual environments for coat protein phenoxyls. *Biochemistry* **1994**, *34*, 1039−1042.

(39) Wen, Z. Q.; Armstrong, A.; Thomas, G. J., Jr. Demonstration by ultraviolet resonance Raman spectroscopy of differences in DNA organization and interactions in filamentous viruses Pf1 and fd. *Biochemistry* **1999**, *38*, 3148−3156.
(40) Arp, Z.; Autrey, D.; Laane, J.; Overman, S. A.; Thomas, G. J., Jr. Tyrosine Raman signatures of the filamentous virus Ff are diagnostic of non-hydrogen-bonded phenoxyls: demonstration by Raman and infrared spectroscopy of *p*-cresol vapor. *Biochemistry* **2001**, *40*, 2522−2529.
(41) Thomas, G. J., Jr. New structural insights from Raman spectroscopy of proteins and their assemblies. *Biopolymers* **2002**, *67*, 214−225.
(42) Taddei, P.; Asakura, T.; Yao, J.; Monti, P. Raman study of poly-(alanine-glycine)-based peptides containing tyrosine, valine, and serine as models for the semicrystalline domains of *Bombyx mori* silk fibroin. *Biopolymers* **2004**, *75*, 314−324.
(43) Tsukada, M.; Freddi, G.; Nagura, M.; Ishikawa, H.; Kasai, N. Structural changes of silk fibers induced by heat treatment. *J. Appl. Polym. Sci.* **1992**, *46*, 1945−1953.
(44) Freddi, G.; Kato, H.; Tsukada, M.; Allara, G.; Shiozaki, H. Physical properties and dyeability of NaOH-treated silk fibers. *J. Appl. Polym. Sci.* **1995**, *55*, 481−487.
(45) Tsukada, M.; Freddi, G.; Monti, P.; Bertoluzza, A.; Shiozaki, H. Physical properties of 2-hydroxyethyl methacrylate-grafted silk fibers. *J. Appl. Polym. Sci.* **1993**, *49*, 1835−1844.
(46) Tsukada, M.; Kasai, N.; Freddi, G. Structural analysis of methyl methacrylate-grafted silk fibers. *J. Appl. Polym. Sci.* **1993**, *50*, 885−890.
(47) Tsukada, M.; Freddi, G.; Ishiguro, Y.; Shiozaki, H. Structural analysis of methacrylamide-grafted silk fibers. *J. Appl. Polym. Sci.* **1993**, *50*, 1519−1527.
(48) Arai, T.; Freddi, G.; Innocenti, R.; Tsukada, M. Preparation of water-repellent silks by a reaction with octadecenylsuccinic anhydride. *J. Appl. Polym. Sci.* **2003**, *89*, 324−332.

BM061017Y